Electronic Supporting Information

Temperature-dependent self-trapped models regulating energy transfer in rare earth double perovskites via $5s^2$ electron doping

Chujun Tan, Shuai Zhang, Haiyan Wang, Jiandong Yao, Hongbang Liu,* Bingsuo Zou,* and Ruosheng Zeng*

State Key Laboratory of Featured Metal Materials and Life-cycle Safety for Composite Structures, School of Physical Science and Technology, Guangxi University, Nanning 530004, China

*Corresponding authors: liuhb@gxu.edu.cn, zoubs@gxu.edu.cn, zengrsh@guet.edu.cn

1. Experiment

1.1 Materials and preparation

Cesium chloride (CsCl, 99.99%), sodium chloride (NaCl, 99.8%), yttrium oxide (Y_2O_3,99.99%), samarium oxide (Sm_2O_3, 99.99%) and antimony butter ($SbCl_3$, 99.99 %) were purchased from Macklin. Hydrochloric acid (HCl, 37 wt% in water) was purchased from Sinopharm Chemical Reagent Co., Ltd. Ethanol anhydrous (CH_3CH_2OH, 99.9%) was purchased from Nanning Blue Sky Experimental Equipment Co., Ltd. All of these chemical agents were used as received without further purification.

Sb^{3+}, Sm^{3+} co-doped Cs_2NaYCl_6 double perovskites were synthesized by a typical solvothermal method. In 25.0-mL Teflon liner, 2.00 mmol of CsCl, 1.00 mmol of NaCl, (1-x)/2 mmol of Y_2O_3, 0.01mmol of $SbCl_3$, x/2 (x=1,2,3,4,5) mmol of Sm_2O_3 and were pre-dissolved in 2.00 mL of HCl by ultrasonication. Then, the mixture was transferred into a stainless steel autoclave and kept at 180 ℃ for 10 h. The Sb^{3+}, Sm^{3+}

co-doped Cs_2NaYCl_6 crystal powders were precipitated and washed three times with ethanol and then dried in an oven at 60 ℃ for 12 h.

1.2 Characterization

The crystal structure was characterized by X-ray powder diffraction (XRD, Bruker D8 Discover). The elemental composition and chemical state were identified by X-ray photoelectron spectroscopy (XPS, Thermo Fisher Scientific ESCALAB 250Xi). The scanning electron microscopy (SEM, Zeiss Sigma 500) was used to observe the morphology. The energy-dispersive spectrometry (EDS, Oxford X-Max Aztec) was used to collect the element composition and distribution. The steady-state PL spectra, photoluminescence quantum yields (PLQY), temperature-dependent PL spectra and temperature-dependent time-resolved PL (TRPL) were measured with a Horiba Jobin Yvon Fluorolog-3 spectrometer. TRPL was also collected using Edinburgh FLS 1000 fluorescence spectrometer. The electronic absorption spectra were measured using a UV-VIS-NIR spectrophotometer (PerkinElmer Instruments, Lambda 750). The OHSP-350M LED Fast-Scan Spectrophotometer was used to evaluate the pc-LED under different drive currents (Hangzhou Hopoo Light&Color Technology Co., Ltd., China). A NIR camera captured the images (EOS 200D, Canon, China). The RL spectra were measured using a Zolix OmniFluo 960SP spectrometer with an FLS-XrayV unit. The down-shifting absolute PLQY of double perovskites was calculated by the formula as following:

$$PLQY = \frac{I_{sample}}{A_{blank} - A_{sample}}$$

Where A_{sample} and A_{blank} are the absorption integral area with and without the double perovskites, and I_{sample} is the down-shifting emission integral area of the double perovskites

1.3 Computational Methods

All calculations using density functional theory (DFT) were carried out using the

Vienna Ab initio simulation package (VASP). The generalized gradient approximation of the Perdew-Burke-Ernzerhof (PBE) parameterization with projector-augmented wave (PAW) method was performed for the exchange and correlation functional. For all elements, including Cs, Na, Y, Sm, Sb and Cl, ultra-soft pseudopotentials were used.

1.4 Fabrication of LED devices

LED devices were fabricated using 365 nm NUV-LED chips. We mixed the powders of 1% Sb^{3+}, 2% Sm^{3+} co-doped Cs_2NaYCl_6 well with epoxy resin respectively. Then, the mixtures are coated on the surface of the LED chip. Finally, the mixture covering the LED chips was put into an oven and dried at 60 ℃ for 72 h to obtain the device.

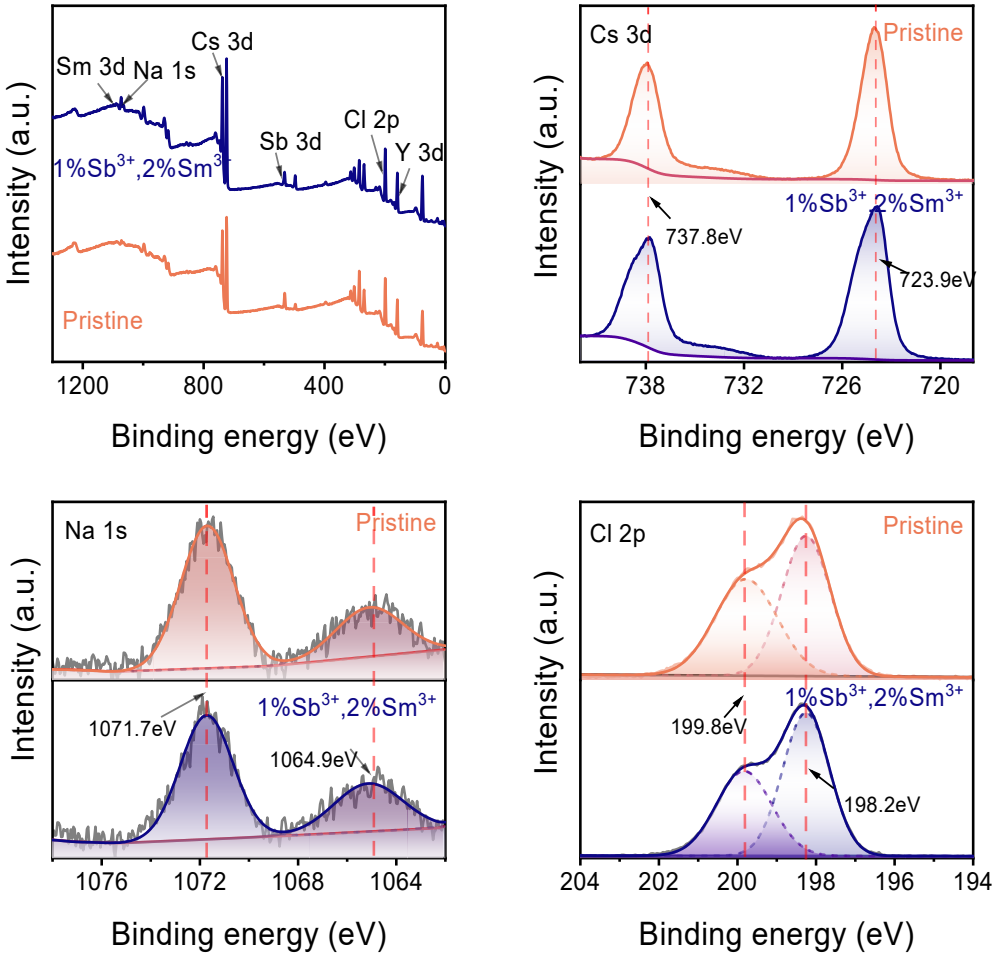

Fig. S1 The high-resolution XPS spectra of Cs 3d, Na 1s and Cl 2p.

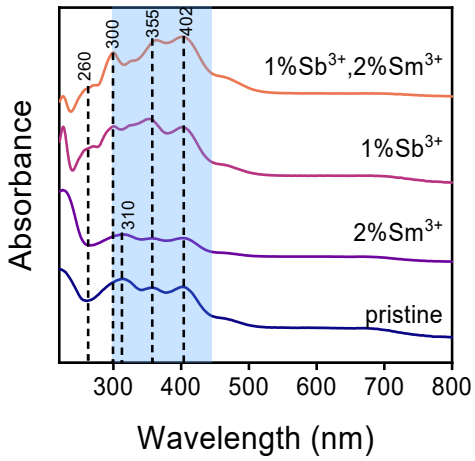

Fig. S2 The absorption spectra of Cs_2NaYCl_6, 1% Sb^{3+}:Cs_2NaYCl_6, 2% Sm^{3+}:Cs_2NaYCl_6 and 1% Sb^{3+}, 2% Sm^{3+} co-doped Cs_2NaYCl_6 double perovskites, respectively.

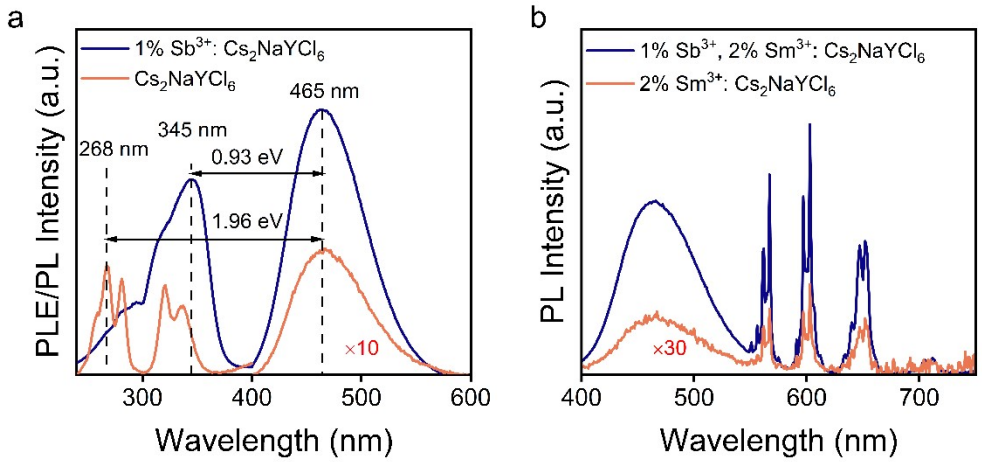

Fig. S3 (a) The PLE and PL spectra of Cs_2NaYCl_6 (Ex@268 nm) and Sb^{3+}:Cs_2NaYCl_6 (Ex@345 nm) double perovskites. (b) The PL spectra of Sm^{3+}, Cs_2NaYCl_6 (Ex@268 nm) and 1% Sb^{3+}, 2% Sm^{3+} co-doped Cs_2NaYCl_6 double perovskites (Ex@345 nm).

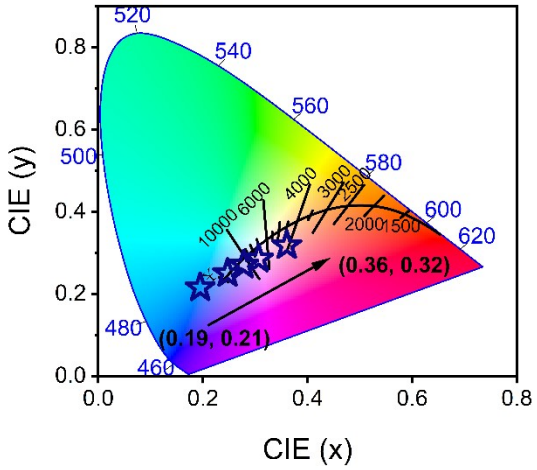

Fig. S4 The CIE of the corresponding samples with different Sm^{3+}-feeding concentrations calculated by CIE 1931.

Table S1. PL lifetimes of 1% Sb^{3+}, x% Sm^{3+} co-doped Cs_2NaYCl_6 (x = 0–5) (emission at 465 nm) with different Sm^{3+}-feeding concentration.

Sm^{3+} concentration	$A_1(\%)$	$\tau_{1(\mu s)}$	$A_2(\%)$	$\tau_{2(\mu s)}$	$\tau_{ave(\mu s)}$
0%	40	0.13	60	1.29	1.22
1%	48	0.10	52	1.27	1.18
2%	57	0.08	43	1.25	1.15
3%	73	0.06	27	1.20	1.04
4%	82	0.05	18	1.14	0.95
5%	87	0.05	13	1.05	0.80

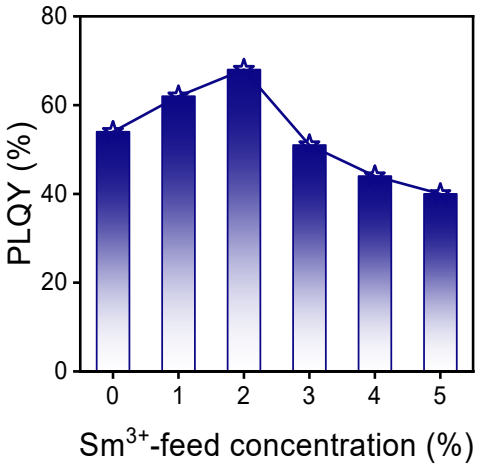

Fig. S5 PLQY evolution of 1% Sb^{3+}, x% Sm^{3+} co-doped Cs_2NaYCl_6 (x = 0, 1, 2, 3, 4, and 5) samples at 345 nm excitation wavelength.

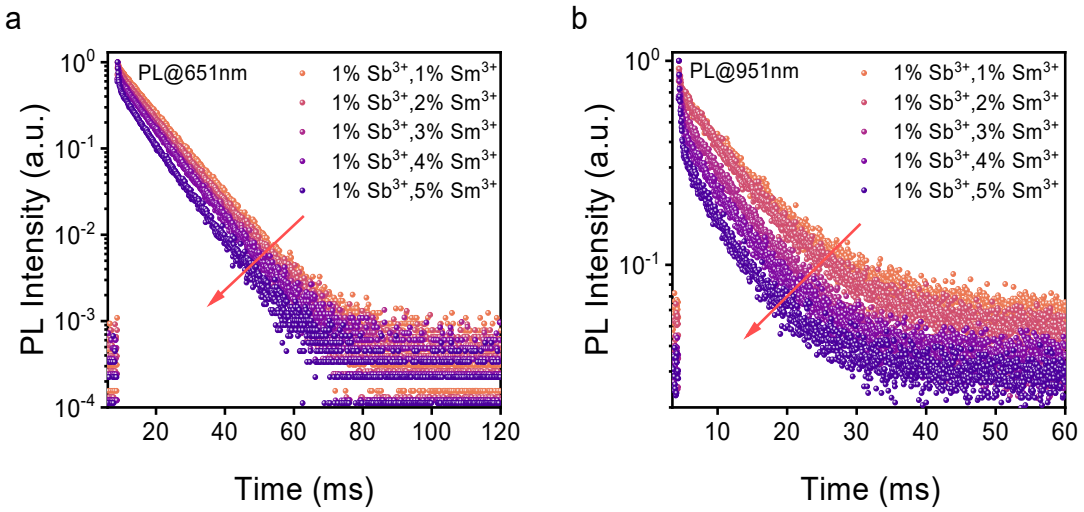

Fig. S6 The PL lifetime of Sb^{3+}, Sm^{3+} co-doped Cs_2NaYCl_6 at (a) 651nm and (b) 951nm.

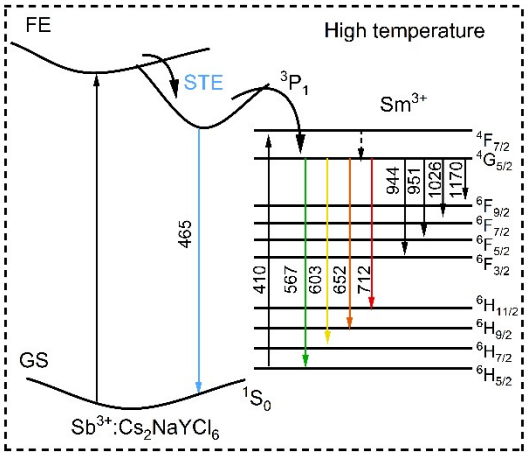

Fig. S7 Schematic diagram of physical mechanism of Sb^{3+}, Sm^{3+} co-doped Cs_2NaYCl_6 double perovskites at high temperature.

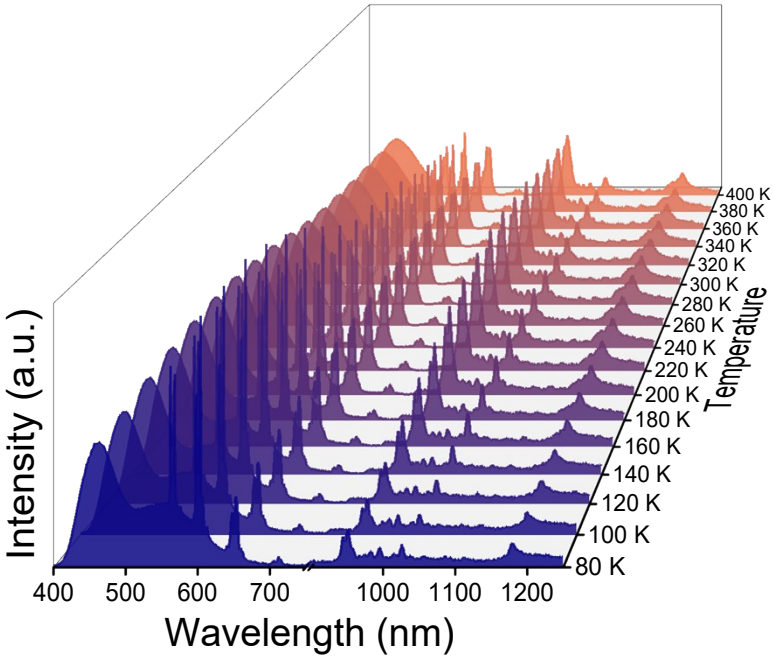

Fig. S8 Temperature-dependent PL spectra of 1% Sb^{3+}, 2% Sm^{3+} co-doped Cs_2NaYCl_6.

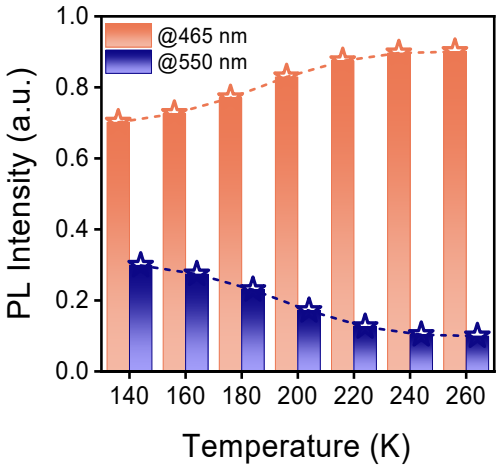

Fig. S9 Changes of PL intensity at 465 and 550 nm with temperatures.

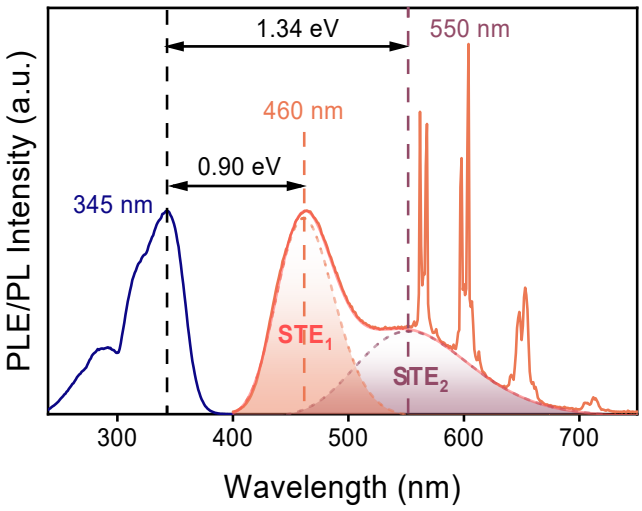

Fig. S10 The PLE and PL spectra of 1% Sb^{3+}, 2% Sm^{3+} co-doped Cs_2NaYCl_6 at low temperature (Ex@345 nm).

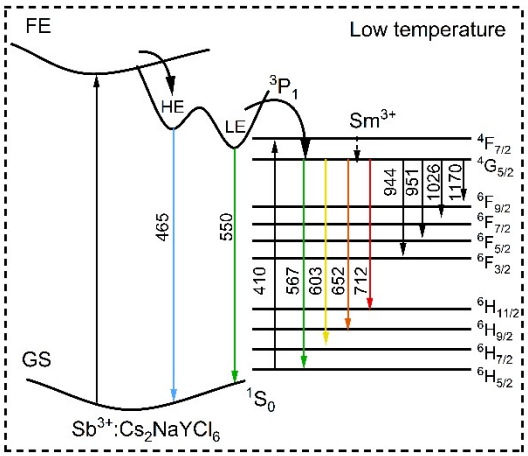

Fig. S11 Schematic diagram of physical mechanism of Sb^{3+}, Sm^{3+} co-doped Cs_2NaYCl_6 double perovskites at low temperature (80–220 K).

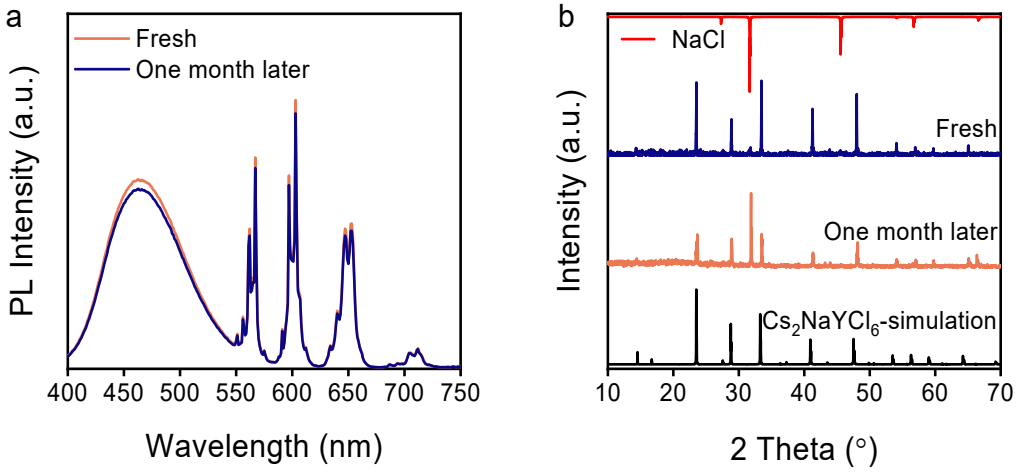

Fig. S12 (a) XRD patterns and (b) PL of 1% Sb^{3+}, 2% Sm^{3+} co-doped Cs_2NaYCl_6 stored in the air for one month.

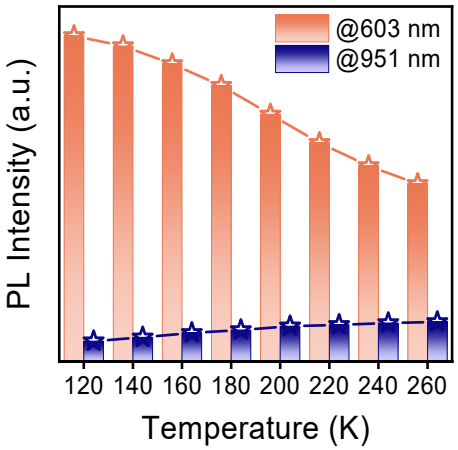

Fig. S13 Corresponding histograms of intensity of Sm^{3+} emission (at 603 and 951 nm) with temperature.

Table S2. Summarized maximum absolute sensitivity (Max. S_a) and maximum relative sensitivity (Max. S_r) values of previously reported rare earth materials.

Materials	Max. $S_{a(K^{-1})}$	Max. $S_{r(\%\ K^{-1})}$	Temperature range (K)	Refs.
Sm^{3+}:Ca_2LaNbO_6	—	0.23	313-573	[1]
Tm^{3+}, Yb^{3+} co-doped $Ba_5Gd_8Zn_4O_{21}$	0.006	0.55	300-510	[2]
Bi^{3+}, Sm^{3+} co-doped $Sr_3Y_2Ge_3O_{12}$	0.0017	0.38	298-498	[3]
$Cs_2NaHo_{0.99}Yb_{0.01}Cl_6$	—	0.68	300-900	[4]
Er^{3+}:$NaLaMgWO_6$	0.0223	1.04	303-483	[5]
Sb^{3+}, Sm^{3+} co-doped $Cs_2NaInCl_6$	0.00173	0.75	140-280	[6]
Sb^{3+}, Sm^{3+} co-doped Cs_2NaYCl_6	0.00141	1.08	120-260	This work

References

1 A. Zhang, Z. Sun, M. Jia, Z. Fu, B. C. Choi, J. H. Jeong and S. H. Park, Sm^{3+}-doped niobate orange-red phosphors with a double-perovskite structure for plant cultivation and temperature sensing, *J. Alloy. Compd.*, 2021, **889**, 161671.

2 H. Suo, C. Guo, Z. Yang, S. Zhou, C. Duan and M. Yin, Thermometric and optical heating bi-functional properties of upconversion phosphor $Ba_5Gd_8Zn_4O_{21}$:Yb^{3+}/Tm^{3+}, *J. Mater. Chem. C*, 2015, **3**, 7379-7385.

3 R. Sun, X. Wei, H. Yu, P. Chen, H. Ni, J. Li, J. Zhou and Q. Zhang, Temperature sensing of $Sr_3Y_2Ge_3O_{12}$:Bi^{3+},Sm^{3+} garnet phosphors with tunable sensitivity, *Dalton Trans.*, 2023, **52**, 2825-2832.

4 Z. Rao, M. Cao, Z. Chen, X. Zhao and X. Gong, Understanding and Effective Tuning of Red-to-Green Upconversion Emission in Ho-Based Halide Double Perovskite Microcrystals, *Adv. Funct. Mater.*, 2024, **34**, 2311568.

5 W. Ran, H. M. Noh, S. H. Park, B. R. Lee, J. H. Kim, J. H. Jeong and J. Shi, Er^{3+}-Activated $NaLaMgWO_6$ double perovskite phosphors and their bifunctional application in solid-state lighting and non-contact optical thermometry, *Dalton Trans.*, 2019, **48**, 4405-4412.

6 X. Li, D. Wang, Y. Zhong, F. Jiang, D. Zhao, S. Sun, P. Lu, M. Lu, Z. Wang, Z. Wu, Y. Gao, Y. Zhang, W. W. Yu and X. Bai, Halide Double Perovskite Nanocrystals Doped with Rare-Earth Ions for Multifunctional Applications, *Adv. Sci.*, 2023, **10**, 2207571.